Publications of the Astronomical Society of the Pacific
108: 419–425, 1996 May

Planetary Nebulae Expansion Distances. III.

ARSEN R. HAJIAN

Department of Astronomy and NAIC, Cornell University, Ithaca, New York 14853 and United States Naval Observatory, USNO/NRL Optical Interferometer Project, 3450 Massachusetts Av. NW, Washington, DC 20392-5420
Electronic mail: hajian@fornax.usno.navy.mil

YERVANT TERZIAN

Department of Astronomy and NAIC, Cornell University, Ithaca, New York 14853
Electronic mail: terzian@astrosun.tn.cornell.edu

Received 1995 August 22; accepted 1995 December 28

ABSTRACT. In a continuing project to determine accurate expansion-parallax distances to planetary nebulae, we have performed high-quality λ6-cm continuum observations of 12 nebulae with the Very Large Array. All of the sources in this imaging survey have one epoch of λ6-cm continuum data in the VLA archives. With two epochs for each planetary nebula, we applied the expansion parallax algorithm. Due in large part to the poor quality of the preexisting epoch, we were successful in only one case (NGC 7662), and obtained a lower limit to the distance for two PNe (Hu 1–2 and NGC 2440). Here, we also present new images acquired in this survey with the intent of reobserving the sample. Similar observations of these nebulae planned in 1997 should be sufficient to detect the expansion of a large percentage of the nebular shells.

1. INTRODUCTION

Distances to astronomical sources are often the subject of considerable controversy and disagreement. For planetary nebulae (PNe) being bright and nearby gives no guarantee of yielding accurate distances. Distances are very important, as they are critical for accurately computing the physical parameters of the nebulae and central stars (mass, luminosity, evolutionary status, birthrate, etc.) and a variety of galactic characteristics (UV radiation, rotation, chemistry, etc.) that can be probed with PNe as test particles. As with any population of generalized objects, it is always possible to do a statistical (or indirect) treatment of an object's property. In the case of PNe, most indirect distance studies assume that the ionized mass is constant throughout the population. While these methods are useful for quantifying bulk characteristics of the PNe population as a whole, they lead to distance errors of ~100% or more for individual nebulae (Terzian 1993; Daub 1982). The relative disagreement between independent and indirect methods of determining distances to PNe have been summarized by Terzian (1993).

A thorough review of all examples of PNe distances computed to date via direct methods is presented by Pottasch (1995). Some direct methods work well for individual sources, but unfortunately distances to most PNe cannot be determined with any but indirect methods. For instance, the central stars of most PNe are too faint for spectroscopic methods and too distant for parallax-based determinations of their distances.

Our approach has been to discard indirect methods as well as methods that involve detailed spectroscopic modeling in favor of a direct, observational test of the nebular distance. We gather direct evidence of the angular expansion of the nebula with respect to time. Typically, PNe expand at speeds ~10 km s^{-1} and, at typical nebular distances of 1 kpc, this translates to an angular expansion rate of only 2 mas yr^{-1}. This is a tiny expansion rate, but if it can be detected, then the distance to the PN can be found by dividing the Doppler velocity of a nebular emission line by the angular expansion rate.

First attempts at detecting nebular angular expansions were performed at optical wavelengths, for example, by Liller et al. (1966) and Liller and Liller (1968). These studies were unfortunately compromised by the long (~1 century) time baseline required between epochs and the different spectral response of the photographic emulsions available.

Recently, however, attempts to detect the angular expansion of PNe at radio wavelengths with the Very Large Array (VLA) have yielded positive results. Using a method known as the *expansion parallax algorithm* to measure nebular ex-

TABLE 1
Epochs 1 and 2 VLA Observations of PNe

Source	RA (1950)	DEC (1950)	$S_{\lambda 6}$ mJy	θ "	$Date_1$	$Array_1$	ref_1	# Vis_2
IC 418[1]	05 25 09.5	−12 44 15	1550	13	08-Aug-82	B	AB156	62813
K3–17[1]	18 53 52.4	+07 03 27	345	8	29-Jul-86	B	AP116	126172
NGC 40[1]	00 10 16.5	+72 14 39	460	36	19-Apr-82	A	AB175	319004
NGC 6826[1]	19 43 27.2	+50 24 12	385	30	15-Feb-83	C	AN020	339753
NGC 6881[1]	20 09 01.0	+37 15 47	180	4	15-Mar-83	C	AI015	78598
IC 5217[2]	22 21 55.6	+50 42 52	163	10	23-Feb-85	A	AH182	209368
NGC 7026[2]	21 04 35.5	+47 39 03	260	30	23-Feb-85	A	AH182	289310
Hb 12[3]	23 23 57.2	+57 54 25	300	4	29-Jul-82	A	AP116	63411
Hu 1–2[4]	21 31 07.0	+39 24 40	155	8	29-Jul-86	B	AP116	211485
NGC 2440[4]	07 39 41.5	−18 05 26	370	18	09-Aug-82	B	AB156	123318
NGC 6543[4]	17 58 34.2	+66 38 05	850	25	27-Mar-89	B	ATO95	170937
NGC 7662[4]	23 23 29.4	+42 15 36	600	20	27-Mar-89	B	AT095	91513

[1] = Class 1 = Unusable Epoch 1 Data.
[2] = Class 2 = Weak Epoch 1 Data.
[3] = Class 3 = Unresolved Epoch 1 Data.
[4] = Class 4 = Fair or Good Epoch 1 Data.

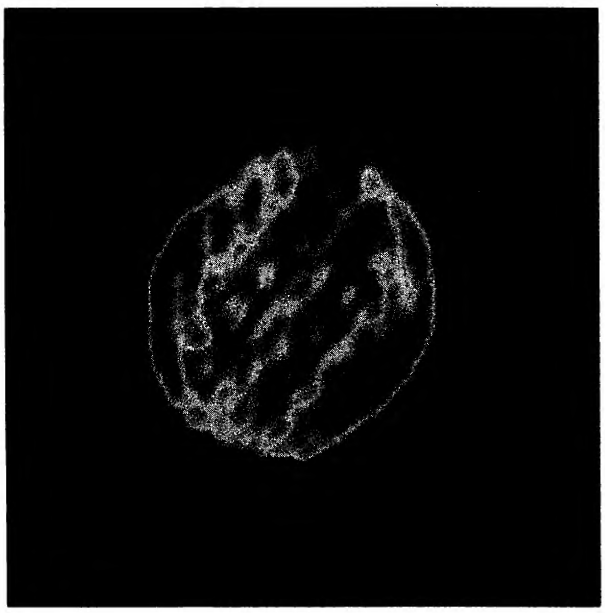

FIG. 1—**[IC 418 Epoch 2]** This is the brightest PN presented in this paper, showing a total flux of 1.29 Jy at λ6 cm. The angular resolution in this image is 1.″24×0.″49. The striped features in the central portion of the nebula are artifacts of the deconvolution process.

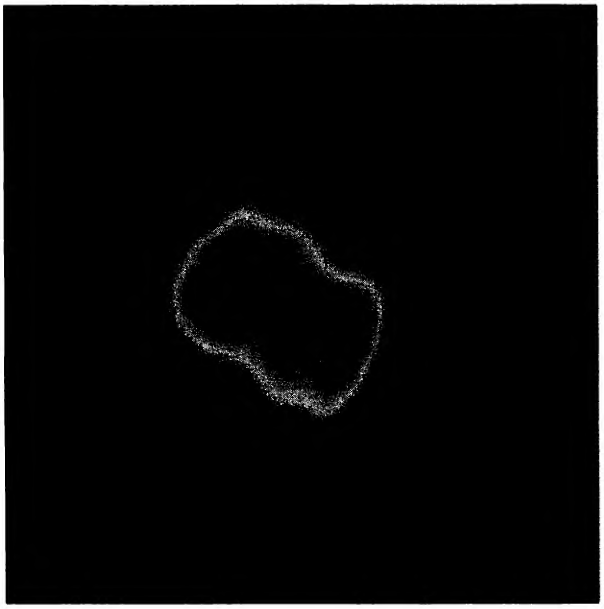

FIG. 3—**[NGC 6881 Epoch 2]**: NGC 6881 is a bipolar PN with the major axis in the SE–NW axis. The angular resolution in this image (0.″38×0.″30) is sufficient to separate the two bright spots on the minor (equatorial) axis. A total flux of 58 mJy is detected.

pansions with two epochs of Fourier data, several authors have achieved success in computing PNe distances with uncertainties as low as 15% (Hajian et al. 1993: *Paper I*; Hajian et al. 1995, *Paper II*; Hajian and Terzian 1995; Masson 1986, 1989a,b; Gomez et al. 1993). The details and numerous advantages of this algorithm have been discussed by the above authors, so we do not repeat the arguments here.

This paper is the third in a series to study the expansion parallax distances for as many PNe as possible. Below we discuss the selection criteria for the survey sample and the resulting expansion parallax distances, and conclude with an assessment of the quality of all existing λ6 cm images of PNe in the VLA archives.

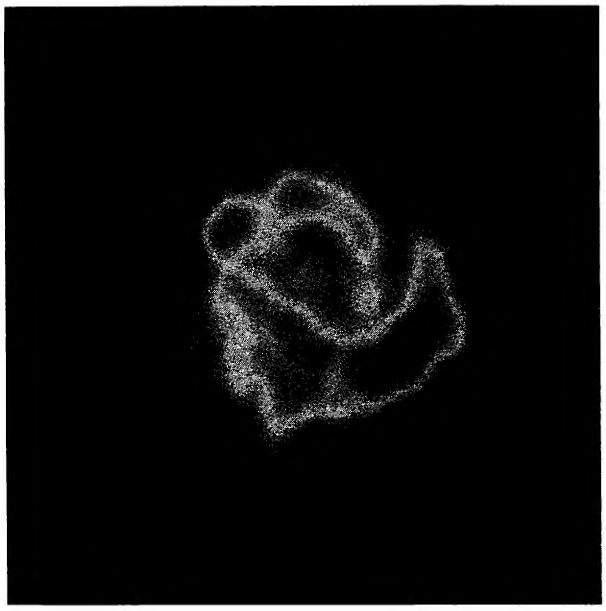

FIG. 2—**[K3–17 Epoch 2]**: The appearance of K3–17 in this image suggests an inclined ring (or spiral?) surrounded by fainter halo gas. The PN is bright ($S_{6\ cm}$=265 mJy) and resolved by the 0.″51×0.″43 beam.

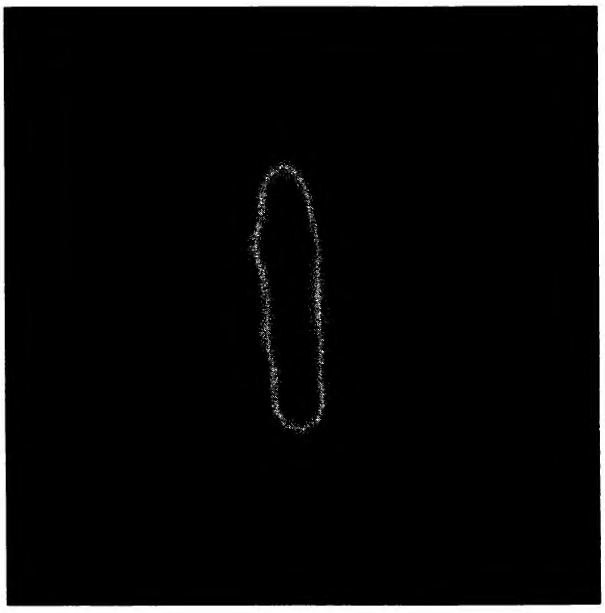

FIG. 4—**[IC 5217 Epoch 2]**: The sharp linear morphology of this PN is unique and bizarre. In fact, the width of IC 5217 is not resolved in the E–W dimension even with a beam of 0.″98×0.″77, although some flux variations are seen in the N–S dimension. A total of 29 mJy is detected in this image.

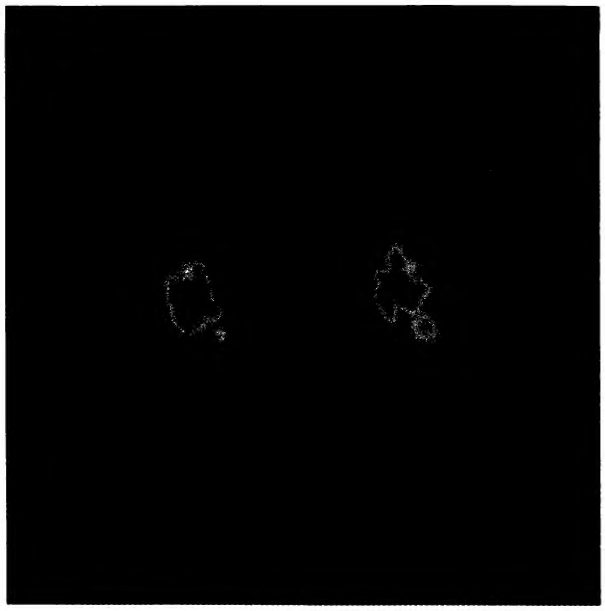

FIG. 5—**[NGC 7026 Epoch 2]**: Similar in appearance to NGC 2440 but weaker (and rotated somewhat), NGC 7026 is seen as two bright regions which correspond to bright equatorial gas. Some real structure may be present in these regions which we have resolved with the 0.″55×0.″47 beam, but it is difficult to be certain due to the faintness of the PN ($S_{6\ cm}$=53 mJy).

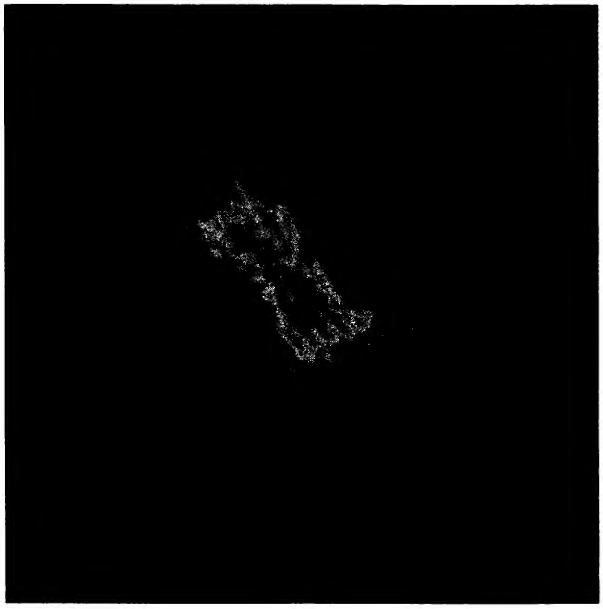

FIG. 7—**[Hu 1-2 Epoch 2]**: This PN appears as a "butterfly" nebula extending in the SW–NE diagonal direction. The clumpiness seen in the image is due to noise resulting from the low average surface brightness of the nebula. The angular resolution in this image is 0.″36×0.″30 and the total detected flux is 26 mJy.

2. OBSERVATIONS

Many of our targets are from the compilation by Zijlstra et al. (1989) and the list in Pottasch (1984), and all have at least one set of continuum observations in the VLA archives at λ6 cm. In order to achieve a sufficient time baseline, we restricted the search to observations prior to 1990. Each source also has an angular diameter greater than 4″ and λ6 cm flux greater than 150 mJy. Our source list is presented in Table 1. The columns are *1*: PN name (NGC, IC, etc.); *2*: RA (equinox 1950); *3*: DEC (equinox 1950); *4*: single-dish λ6 cm flux; *5*: angular diameter; 0″ *6*: Epoch 1 date; *7*: Epoch 1

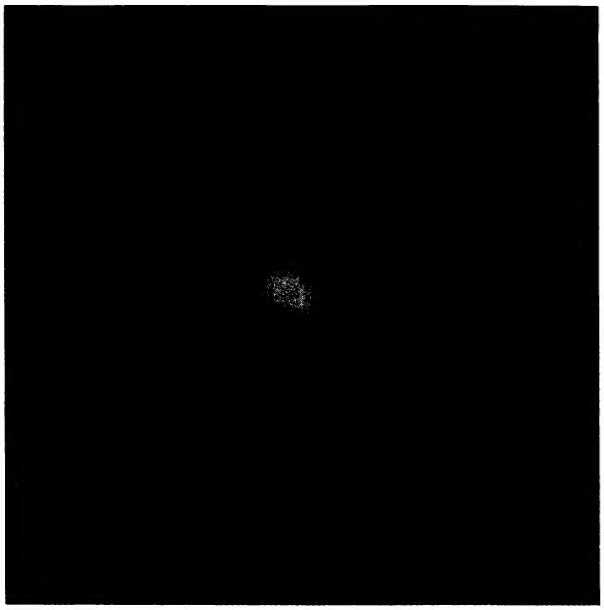

FIG. 6—**[Hb 12 Epoch 2]**: The morphology of this PN is that of a dim point-like nebula with two faint "antennae" extending in the NW and SW directions. The angular resolution is 0.″95×0.″29 and the total detected flux is 26 mJy.

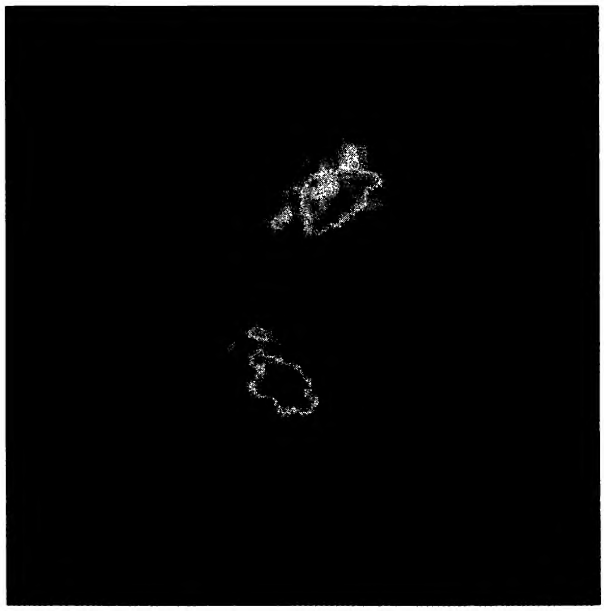

FIG. 8—**[NGC 2440 Epoch 2]**: The high angular resolution in this image of NGC 2440 (0.″54×0.″39) reveals structure in the bright equatorial regions of the nebula. The integrated flux is 109 mJy.

FIG. 9—**[NGC 6543 Epoch 2]**: The angular resolution of this image is (1.″10×0.″32) sufficient to show detailed emission structures in the nebula and the total detected flux is relatively high (272 mJy). The loops are fractured in this image, similar to the [O III] image presented by Harrington and Borkowsky (1994).

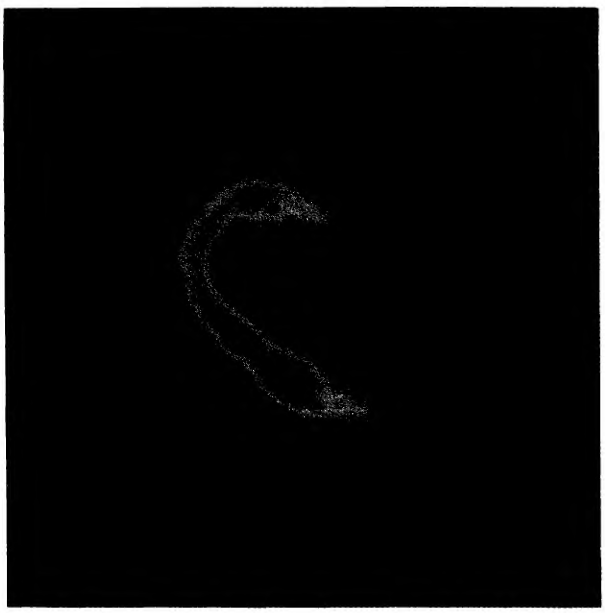

FIG. 10—**[NGC 7662 Epoch 1]**: This is an image of NGC 7662 made with an angular resolution of 1.″42×1.″02. The halo of this PN is barely detected surrounding the brighter ring in the center and the diagonal halo feature in the SE part of the image is real. The total detected flux is 198 mJy.

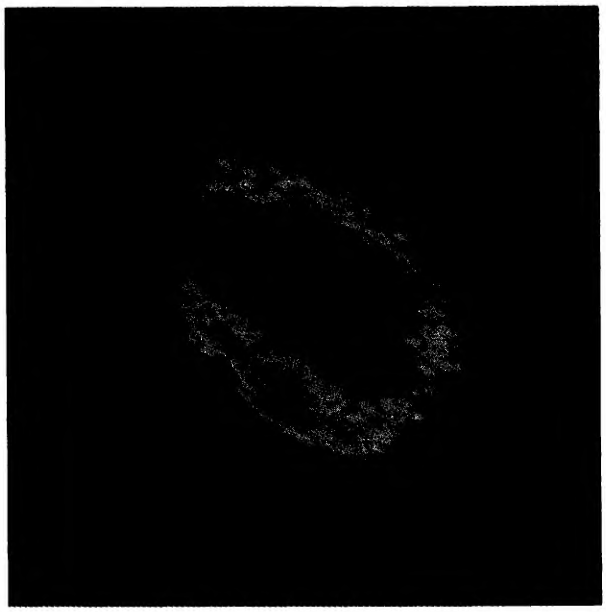

FIG. 11—**[NGC 7662 Epoch 2]**: The improved angular resolution in this image (0.″97×0.″32) as compared to Fig. 10 comes at the price of a lower signal-to-noise ratio. The halo is present in the image, but at a very low level. A total of 177 mJy is detected.

VLAarray configuration; *8*: VLA Archive reference; *9*: Number of epoch 2 visibilities. The epoch 2 observations were made by us in 1994 April at the VLA operating at a wavelength of λ6 cm and bandwidth of 50 MHz in the A array. Observing conditions were excellent, and most of the nebulae were easily located and detected. Source observations were interleaved with secondary calibrators to measure the phase stability of the array.

All data were calibrated with the usual post-processing techniques using 3C286 and 3C84 as primary calibration sources. We then applied several passes of phase, then phase and amplitude self-calibration to minimize noise residuals and to achieve a high dynamic range in the resulting images. We display the deconvolved maps for epoch 2 for most nebulae and epochs 1 and 2 for NGC 7662 in Figs. 1–11. The greyscale transfer function at the top of each map is calibrated in mJy/beam for bright sources and μJy/beam for weaker ones.

3. RESULTS

With the exception of the weak source NGC 6826 and the large nebula NGC 40, all of the epoch 2 images were good detections and were successfully deconvolved, as can be seen in the figures. Unfortunately, most of the epoch 1 data are of marginal quality: of the 12 PNe listed in Table 1, 5 have poor or defective data and were unusable, 2 have detectable but very weak signals, 1 source is unresolved, and 4 have fair or good quality images.

We completed processing the data from the final four sources using the cross-calibration method described extensively in Papers I and II. We made difference maps for each of the Class 4 sources and Fig. 12 shows the results for NGC 7662.

4. DISCUSSION OF INDIVIDUAL NEBULAE AND THEIR DISTANCES

4.1 Hu 1–2

Hu 1–2 appears as a 6″×2″ butterfly-like structure in our radio maps. Our radio image correlates very well with the optical Hα+[N II] line map published by Sabbadin et al. (1987). The structure we have imaged has been interpreted by the above authors as a dense waist or toroid surrounding the central star. Several indirect distance computations to Hu 1–2 exist in the literature. The Shklovsky distances calculated by Cahn et al. (1992: CKS) and Daub (1982), as well as the extinction distances of Pottasch (1983) and Sabbadin (1986) are all near 1.5 kpc.

Although Sabbadin et al. (1987) were able to measure the expansion velocities from a number of emission lines, no accurate spatial models exist. Therefore, we assume that the torus is approximately circular and that the tangential and radial velocities are equal. We use an average of the [O III], Hα, and [Ar III] (28.5, 22.5, and 28.5 km s^{-1}, respectively) expansion velocities to adopt v_{exp}=26±9 km s^{-1}. The large error bars are to accommodate the uncertainty in the source geometry, as is done in Papers I and II. Although we did not detect the characteristic signature confirming the expansion in the difference map, we can constrain the upper limit of the angular expansion rate. Our calculations yield a maximum expansion rate of 4.7 mas yr^{-1}, which indicates that the minimum distance to Hu 1–2 is 1.17 kpc. This value is less than almost all estimates of the distance to Hu 1–2, which is reassuring.

4.2 NGC 2440

This nebula is morphologically similar to Hu 1–2, exhibiting a butterfly-like appearance with a central ring. The image of NGC 2440 in Fig. 8 is actually the core of a more extended nebula which we could not image since it is larger than the size probed by the smallest baseline in the A array. The totality of the nebula (which has a size of ≈1′) can be seen in images by Balick (1987). Using various modifications of the Shklovsky method, several previous studies have computed distances which are mostly in excess of 1 kpc. For example, CKS derive a distance of 1.3 kpc and Daub (1982) finds 1.1 kpc. However, these results are in conflict with the 500 pc distance based on the detailed spectroscopic modeling of the nebula (Baessgen et al. 1995).

The recently published model of NGC 2440 (Baessgen et al. 1995) describes the PN as a cylinder with the symmetry axis along the plane of the sky, and agrees very well with the observed optical brightness distribution. Although this model also predicted emission-line fluxes and spectroscopic characteristics of the nebula that are in good agreement with observation, there was little information published specifically about the inner torus that we have imaged. As a result, we assume (as in the case of Hu 1–2) that the radial and tangential expansion velocities of the inner core are equal.

It is not easy to adopt an expansion velocity of the inner region of NGC 2440, since no spatially resolved studies exist. The lack of agreement among authors who have measured the expansion velocity of NGC 2440 (even for the same ion!) and the complex source geometry further complicate this situation. The highest quality data comes from the 3 km s^{-1} resolution observations of Bianchi (1992). She finds that $v_{exp}(H)$=18.7 km s^{-1} by fitting a pair of Gaussian profiles to the Hα observed line for the inner parts of the nebula (where the nebular motion is mostly radial). Also using the Hα line, Louise and Pascoli (1985) derived the much larger value of 28 km s^{-1}. Two determinations of v_{exp}(O III) exist, and these are the only consistent values in the literature. Wilson (1950) and Meatheringham et al. (1988) both find v_{exp}(O III)=33 km s^{-1}. The orientation of the inner region was only tentatively examined by Kaler and Aller (1975), who modeled the region as two bright condensations tilted by 60° relative to the line of sight. We adopt an expansion velocity of 24±8 km s^{-1} to account for the relative paucity of and inconsistencies in the data.

We did not detect the angular expansion of NGC 2440 in the difference map and based on the noise level in the map and the shell gradient, we compute a maximum angular expansion rate of 4.4 mas yr^{-1} and a minimum distance to NGC 2440 of 1.1 pc.

4.3 NGC 6543

NGC 6543 is a very complicated nebula which has recently been the subject of renewed activity (for example, Harrington and Borkowsky 1994; Patriarchi and Perinotto 1995). We do not attempt to summarize the rich observational history in the literature for this object. We only note in passing that a λ6 cm image has been published (Balick et al. 1987), but the quality of the image is not sufficient for an expansion parallax study. Shklovsky distances to NGC 6543 are relatively close: 0.98 kpc was found by CKS and 0.64 kpc by Daub (1982).

Due to the large number of individual spatial and velocity features, a model of NGC 6543 is critical in order to avoid large errors in the expansion velocity. Kinematic models based on more than 30 longslit spectra from NGC 6543 are presented by Miranda and Solf (1992). They find that the expansion velocity varies by a factor of ≈2 (about 15–30 km s^{-1}) between the inner and outer equatorial regions. In addition, the polar expansion velocities are a factor of ≈2 greater than the equatorial velocities.

Unfortunately, our best attempts to apply the expansion algorithm to this PN failed. We believe that this is due to the variety of distinct features (the algorithm works best on smooth extended regions) and to the difference in array configurations between epochs. We would like to note that the problem is not caused by subtracting features that have different convolved widths in each epoch: angular-resolution disparities are irrelevant since only regions in the UV plane which are common to both epochs are considered in the subtraction. The problem is caused by small interpolation errors which become significant when comparing two epochs with differing UV coverage. Furthermore, NGC 6543 shows evidence of significant structure on small scales which are resolved in the epoch 2 images but not in the epoch 1 images. The angular-expansion algorithm fails in such circumstances, as any putative expansion signature is most often lost in the artificial structure that is generated when unresolved components are subtracted from their corresponding resolved features in the other epoch.

4.4 NGC 7662

NGC 7662 is a bright nebula which exhibits an elliptical ring surrounded by a fainter spherical halo. This structure is characteristic of many PNe (e.g., NGC 2392 and NGC 3242). Shklovsky distances to this PN have been found by several authors including CKS (0.84 kpc) and Daub (1982) (1.15 kpc). The halo is interesting because it has a significantly hotter electron temperature than the inner ring, which may be indicative of shocks being driven into the halo gas (see Middlemass et al. 1989; 1991). Although we discuss the halo in a future paper (Hajian et al. 1995), it is the inner ring which is the focus of this section since the expansion algorithm works best with well-detected features that are radially peaked and that we can assume to be expanding radially from the central source with a single velocity. The optical observations of [O III] and Hα by Wilson (1950) and Osterbrock et al. (1966) are all consistent at about 26±3 km^{-1}. Weedman (1968) fit a spatiokinematic model to [O III] and Hα spectra obtained along the major axis. He concludes that the inner ring has an axial ratio of 3:2 and that the major axis is inclined by 50° with respect to the line of sight. We assume that the ratio of the major/minor axis velocities are inversely proportional to their axial ratio (i.e., all of the ring material began at the central star at some time), and after correcting for projection effects, we conclude that the tangential expansion velocity of the minor axis is 21±7 km s^{-1}.

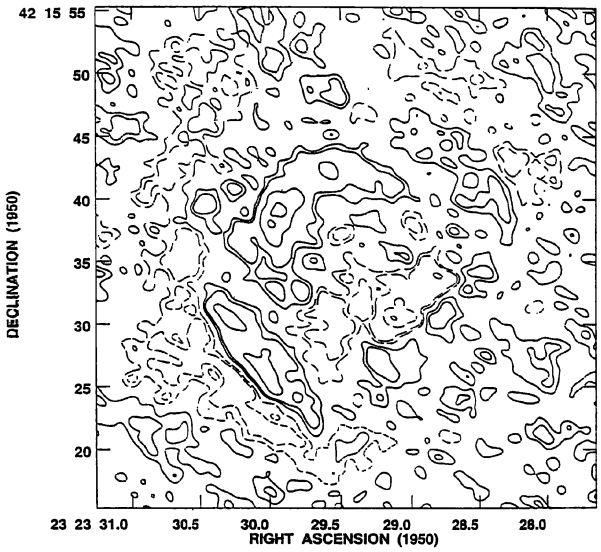

FIG. 12—**[NGC 7662 Difference Map]**: This map was computed by slightly shifting the images in Figs. 10 and 11 relative to one another and (effectively) subtracting them using the Expansion Parallax Algorithm. The difference features are close to the noise level, but cuts parallel to the minor axis reveal a detectable $\dot{\theta}$. The noise level in this map is 0.082 mJy/beam.

We shifted the data from one epoch by 0.″2 relative to the other epoch in order to align the images and to minimize spurious signatures in the difference map. The map displayed in Fig. 12 represents our best effort to subtract the two epochs, and a careful inspection of the difference map reveals the faint characteristic signature of radial expansion along the minor axis. We examined the brightness profiles in one dimensional cuts parallel to the minor axis of the ring and analysis of these yields an angular expansion rate of 5.6±5.0 mas yr^{-1}. When combined with the kinematics and nebular model above, we conclude that the parallax distance to NGC 7662 is 0.79±0.75 kpc. The large error in this estimate is due mainly to the faintness of the difference features. We do not attempt to rule out competing distance estimates in the literature because of our uncertain determination.

5. SUMMARY AND CONCLUSIONS

Despite detecting only one expansion signature in our survey, we have obtained good λ6 cm detections of most of the program nebulae and, in most cases, our maps have the highest resolution and are the best quality images available at radio wavelengths. Future observations are required to determine distances to the PNe in Table 1. High-priority sources (those that are bright and have shallow shell gradients and large expansion velocities) can be reobserved as early as 1997, and by 1999 the nebular expansion of the majority of

the remainder can be detected. In addition, these observations highlight the advantage (and in some cases the requirement) that both epochs be performed in as similar antenna configurations as possible. Also, now that high-quality epochs of some PNe exist in multiple VLA array configurations (such as the A and B array observations of NGC 6543), it would be useful to obtain a future epoch in both configurations. We also point out that observations in the spirit of Miranda and Solf (1992) for NGC 6543 or O'Dell et al. (1990) for NGC 2392 are ideal for an expansion parallax study, and we hope that more spatial and kinematic models of PNe will be devised based on multiple longslit observations with high spectral resolution.

As a result of this study we have detected the expansion of NGC 7662, bringing the total number of PNe with expansion distances to 8. We have also determined lower limits for the distances to the PNe NGC 2440 and Hu 1–2.

We would like to thank the generosity of the VLA telescope operators and especially the support offered by the VLA technical staff. We also wish to acknowledge the valuable contributions of Carl Bignell, who helped extract data from the VLA archives, and J. van Gorkom and J. Hibbard who contributed during the epoch 1 observations of NGC 7662 and NGC 6543. This work was supported in part by the National Astronomy and Ionosphere Center, which is operated by Cornell University under a cooperative agreement with the National Science Foundation. The National Radio Astronomy Observatory is operated by Associated Universities, Inc., under a cooperative agreement with the National Science Foundation.

REFERENCES

Balick, B. 1987, AJ, 94, 671
Balick, B., Bignell, C. R., Hjellming, R. M., and Owen, R. 1987, AJ, 94, 948
Baessgen, M., Diesch, C., and Grewing, M. 1995, A&A, 297, 828
Bianchi, L. 1992, A&A, 260, 314
Cahn, J. H., Kaler, J. B., and Stanghellini, L. 1992, A&AS, 94, 399
Daub, C. T. 1982, ApJ, 260, 612
Gomez, Y., Rodriguez, L. F., and Moran, J. M. 1993, ApJ, 416, 620
Hajian, A. R., Terzian, Y., and Bignell, C. 1993, AJ, 106, 1965 (Paper I)
Hajian, A. R., Terzian, Y., and Bignell, C. 1995, AJ, 109, 2600 (Paper II)
Hajian, A. R., and Terzian, Y. 1995, in Asymmetric Planetary Nebulae, ed. A. Harpaz and N. Soker, Ann. Israel Phys. Soc., 11, 142
Hajian, A. R., Balick, B., and Terzian, Y. 1995, in preparation
Harrington, J. P., and Borkowsky, K. J. 1994, BAAS, 26, 1469
Kaler, J. B., and Aller, L. H. 1975, PASP, 86, 635
Liller, M. H., Welther, B. L., and Liller, W. 1966, ApJ, 144, 280
Liller, M. H., and Liller, W. 1968, Planetary Nebulae, ed. D. Osterbrock and C. R. O'Dell (London, Reidel)
Louise, R., and Pascoli, G. 1985, A&A, 150, 285
Masson, C. R. 1986, ApJ, 302, L27
Masson, C. R. 1989a, ApJ, 336, 294
Masson, C. R. 1989b, ApJ, 346, 243
Meatheringham, S. J., Wood, P. R., and Faulkner, D. J. 1988, ApJ, 334, 862
Middlemass, D., Clegg, R. E. S., and Walsh, J. R. 1989, MNRAS, 239, 1
Middlemass, D., Clegg, R. E. S., Walsh, J. R., and Harrington, J. P. 1991, MNRAS, 251, 284
Miranda, L. F., and Solf, J. 1992, A&A, 260, 397
Osterbrock, D. E., Miller, J. S., and Weedman, D. W. 1966, ApJ, 145, 697
O'Dell, C. R., Weiner, L. D., and Chu, Y. H. 1990, ApJ, 362, 226
Patriarchi, P., and Perinotto, M. 1995, A&AS, 110, 353
Pottasch, S. R. 1984, in Planetary Nebulae, IAU Symposium No. 104, ed. D. R. Flower (Dordrecht, Reidel)
Pottasch, S. R. 1995, A&A, preprint
Sabbadin, F. 1986, A&AS, 64, 579
Sabbadin, F., Cappallaro, E., and Turatto, M. 1987, A&A, 182, 305
Terzian, Y. 1993, in Planetary Nebulae, IAU Symposium No. 155, ed. R. Weinberger and A. Acker (Dordrecht, Kluwer), p. 109
Weedman, D. 1968, ApJ, 153, 49
Wilson, O. C. 1950, ApJ, 111, 279
Zijlstra, A. A., Pottasch, S. R., and Bignell, C. 1989, A&AS, 79, 329